

***In situ* detection of two ferromagnetic resonance modes in coupled Ni/Cu/Co/Cu(001) trilayer structures**

J. Lindner,* Z. Kollonitsch, E. Kosubek, M. Farle,[†] and K. Baberschke

Institut für Experimentalphysik, Freie Universität Berlin, Arnimallee 14, D-14195 Berlin, Germany

(Received 25 August 2000; published 9 February 2001)

Ultrathin Ni and Co films, separated by Cu spacer layers with thicknesses in the range 4–15 monolayers, are prepared and measured *in situ* via ferromagnetic resonance (FMR) between 50 and 400 K. Due to the interlayer exchange coupling two resonance modes are observed, corresponding to in- and out-of-phase precession of the rf magnetizations in the two magnetic layers, i.e., the acoustic and optic mode. The fields for resonance H_{res} and the linewidths ΔH_{pp} of the exchange coupled FMR modes are measured as a function of temperature. Since all the measurements are performed *in situ*, we can compare the signal of the first (bottom) magnetic layer before and after the evaporation of the second (topmost) one. For the coupled films we observe an increase of ΔH_{pp} compared to the uncoupled case. From the shift of H_{res} after the deposition of the second layer the sign and relative strength of the coupling is derived.

DOI: 10.1103/PhysRevB.63.094413

PACS number(s): 75.70.-i, 76.50.+g, 75.30.Et

INTRODUCTION

Interlayer exchange coupling between ferromagnetic layers mediated by a nonmagnetic spacer plays a key role for understanding many properties observed in magnetic materials. Therefore trilayers, like the ones being used in our experiments, can be considered as prototype systems. An experimental method that has been widely used to investigate the exchange coupling in trilayers is ferromagnetic resonance (FMR). Among other techniques, FMR has been proven to be a powerful tool, since it allows for the determination of the exchange coupling strength in ferro- and antiferromagnetically coupled systems,^{1–8} as well as the internal anisotropy energies⁹ in one experiment. Although a lot of work was done in applying the FMR technique to the field of trilayers, there are still open questions. In all investigations up to now the trilayers were prepared under ultrahigh vacuum conditions, but the FMR measurements themselves were done *ex situ*. The latter requires that the samples have to be capped by nonmagnetic protective layers. Two questions immediately arise: (i) What is the influence of the protective layer? Especially for ultrathin films, surface effects are very important and therefore capping-layers often have strong effects on the magnetic properties of the underlying magnetic layers. (ii) What are the differences of the magnetic properties in the coupled case compared to the uncoupled one? The latter question is not only interesting from the experimental point of view but also important for testing the predictions of theory dealing with FMR in coupled trilayers. While question (i) has been discussed,¹⁰ question (ii) could not be addressed up to now.

Here we present *in situ* FMR measurements on Ni/Cu/Co/Cu(001) trilayer structures and examine in a first step the uncoupled Cu/Co/Cu(001) system. After evaporating the second (Ni) magnetic layer we study the influence of the exchange coupling *in situ*. The paper is organized as follows. In Sec. II we review the theoretical background of FMR in trilayers. Section III explains the structural properties of the investigated trilayer structures and our *in situ* FMR appara-

tus, while Sec. IV shows the FMR spectra and discusses the main experimental results.

SPIN-WAVE DISPERSION IN COUPLED TRILAYERS

The geometry and coordinate system employed in this investigation is depicted in Fig. 1(a). We consider two ferromagnetic layers A, B of thickness d_A, d_B which are separated by a nonmagnetic Cu spacer layer of thickness d_{Cu} . The coordinate system is chosen so that the xy plane is parallel to the film plane, with the y axis pointing along the $[110]$ direction. The $[001]$ direction along the film normal is chosen to be the z axis. The external magnetic field \vec{H} is applied in the yz plane at a variable angle θ_H with respect to the $[001]$ -axis being always perpendicular to the driving microwave field \vec{H}_{rf} . Since the $[110]$ in-plane direction is the easy axis for Co as well as for Ni films within the thickness range in this work,^{11,12} the equilibrium directions of the two magnetizations \vec{M}_A and \vec{M}_B are confined to the yz plane and can be characterized by two polar angles θ_A and θ_B .

The theoretical background presented here is based on Refs. 2, 5, and 7. The equilibrium directions of \vec{M}_A and \vec{M}_B are determined by the minima of the free energy per unit area F . F includes several contributions:

$$F = F_Z + F_A + F_{dip} + F_{exch}. \quad (1)$$

F_Z is the Zeeman energy per unit area and can be written as

$$F_Z = - \sum_{i=A,B} d_i \vec{M}_i \cdot \vec{H}. \quad (2)$$

F_A is the uniaxial anisotropy energy which has the form

$$F_A = - \sum_{i=A,B} \frac{d_i}{M_i} (\vec{M}_i \cdot \vec{e}_z)^2 \cdot \frac{1}{2} H_{u,i}. \quad (3)$$

$H_{u,i} = 2K_{2,i}/M_i$ is the uniaxial anisotropy field and \vec{e}_z is the unit vector along the z axis, so that $\vec{M}_i \cdot \vec{e}_z = M_i \cdot \cos \theta_i$ are the components of the magnetizations in the z direction, i.e.,

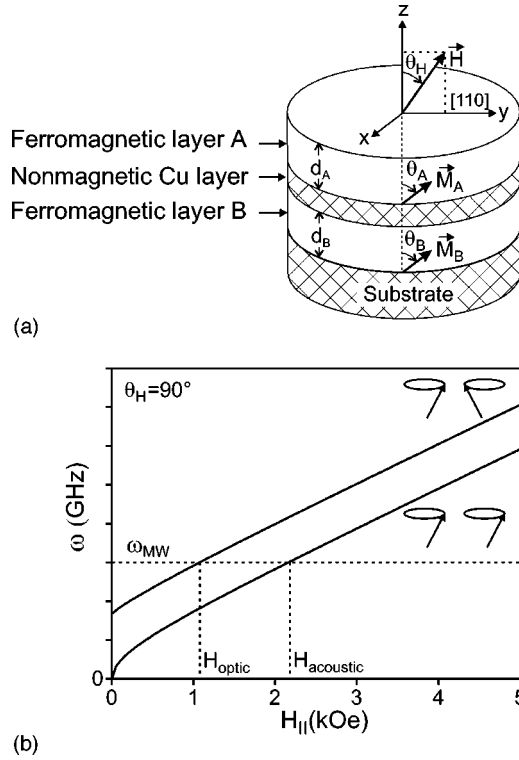


FIG. 1. (a) The coordinate system used in the measurements and the definition of angles for the trilayer systems. (b) The dispersion relation for a symmetric ferromagnetically coupled trilayer. The external field is applied parallel to the film plane, i.e., $\theta_H=90^\circ$, which is the easy direction of the system. The upper branch is the relation for the optic mode (both magnetizations resonate out of phase) whereas the lower branch shows the $\omega(H)$ dependence of the acoustic mode (the magnetizations precess in-phase). ω_{MW} indicates the microwave frequency level, i.e., in our case $\omega_{MW}=9\text{GHz}$. The fields for resonance of the optic (H_{optic}) and the acoustic mode (H_{acoustic}) are given by the points where the microwave level crosses the dispersion curves.

along the uniaxial axis. In our notation $H_{u,i}>0$ indicates a preferential orientation of the M_i along the uniaxial axis, i.e., along the film normal, whereas $H_{u,i}<0$ leads to an energy minimum, if the M_i are in the film plane.

F_{dip} is the dipolar demagnetizing energy,

$$F_{\text{dip}} = \sum_{i=A,B} \frac{d_i}{M_i} (\vec{M}_i \cdot \vec{e}_z)^2 \cdot \frac{1}{2} H_{\text{dip},i}. \quad (4)$$

$H_{\text{dip},i} = -4\pi M_i$ are the demagnetizing fields of the two layers resulting from the magnetic charge density that develops if the magnetizations are rotated out of the film plane. As a consequence F_{dip} always has its minimum for the M_i lying in the film plane. Since our films can be treated in a good approximation as thin discs, the demagnetizing field along the film plane is negligible, so that only the magnetization components along the film normal $\vec{M}_i \cdot \vec{e}_z$ have to be taken into account.

F_{exch} is the exchange energy,

$$F_{\text{exch}} = -J_{AB} \frac{\vec{M}_A \cdot \vec{M}_B}{M_A M_B}. \quad (5)$$

J_{AB} is the interlayer exchange coupling constant. By convention, positive values of J_{AB} indicate ferromagnetic coupling whereas negative ones antiferromagnetic coupling.

Using the polar coordinate system shown in Fig. 1(a), the free energy per unit area can be written as

$$F = \sum_{i=A,B} d_i \{ -HM_i \cos(\theta_i - \theta_H) + \cos^2 \theta_i [2\pi M_i^2 - K_{2,i}] \} \quad (6a)$$

$$- J_{AB} \cos(\theta_A - \theta_B). \quad (6b)$$

Once the equilibrium angles of the two magnetizations \vec{M}_i are determined for all values of the magnetic field \vec{H} , the dispersion relation, i.e., the dependence of the microwave frequency ω on the resonance field H_{res} , can be derived. Usually this is done following the approach of Smit and Beljers,¹³ which has been extended to trilayer structures (see, for example, Refs. 2, 5, and 8). To visualize the results of the theory we give a simplified example that demonstrates the main features of FMR on trilayers. The case of a symmetric ($K_{2,A}=K_{2,B}$ and $d_A=d_B=d$) ferromagnetically coupled ($J_{AB}>0$) trilayer is assumed, but the basic results can be extended also to the asymmetric case. The dispersion relation for this symmetric situation⁵ is shown schematically in Fig. 1(b). One FMR mode, the acoustic mode, corresponds to the rf components of the two magnetizations resonating in phase, the other mode corresponds to the so-called optic mode, where the rf components are resonating out of phase. Since for the acoustic mode and for the case of ferromagnetic coupling no contribution to the resonance condition, i.e., no torque on the \vec{M}_i , is produced, the dispersion relation for the acoustic mode does not change upon coupling compared to the case of a single ferromagnetic layer. This is not necessarily the case for asymmetric trilayers. In such systems also the acoustic mode differs from the single layer case. The optic mode on the other hand introduces an additional internal field to the dispersion relation. This field is in the case of the symmetric ($d_A=d_B=d$ and $M_A=M_B=M$) ferromagnetically coupled trilayer given by

$$H_{\text{exch}} = \frac{-2J_{AB}}{d \cdot M}. \quad (7)$$

As a result, the optic mode is shifted with respect to the acoustic mode by a value of H_{exch} . Since J_{AB} was assumed to be positive, one observes the optic mode for the same frequency at lower values of the external field H . For stronger coupling the shift becomes larger. For asymmetric trilayers this still is true, but the value of the shift is not given anymore by the simple Eq. (7).

In the case of an antiferromagnetically coupled system the optic mode is at the higher fields with respect to the acoustic one. This is due to the decrease of the exchange energy when the two magnetizations are not aligned parallel. In the general case of an asymmetric trilayer it has been shown^{5,14} that,

even if both modes are shifting compared to the single layer case, they always shift in the same direction. For ferromagnetically coupled systems both modes shift to smaller fields, whereas for antiferromagnetic coupling both modes shift to higher field values.

EXPERIMENTAL DETAILS

As substrate a Cu(001) single-crystal disk, 5 mm in diameter, was used. The surface was prepared by cycles of sputtering with Ar^+ ions and annealing to ~ 900 K. Details of the substrate preparation can be found in Ref. 15. After inserting the crystal into the ultrahigh vacuum chamber with a base pressure $< 1 \times 10^{-10}$ mbars and at least 15 sputter cycles the surface showed sharp low-energy electron-diffraction (LEED) patterns and no detectable contamination in the Auger electron spectra.

The magnetic layers (Ni and Co) were evaporated at a pressure $< 4 \times 10^{-10}$ mbars whereas the pressure during evaporation of the Cu spacer layers was stabilized below 6×10^{-10} mbars. For all trilayers the magnetic layer thicknesses were kept constant [7 monolayers (ML's) of Ni and 2 ML's Co]. The Cu spacer thickness was varied for the different samples in the range 4–15 ML's, in order to change the strength of the interlayer exchange coupling. The rate during evaporation, i.e., the time per ML equivalent, was 120 s/ML for Ni, 330 s/ML for Co, and 280 s/ML in the case of Cu. All evaporations were carried out at temperatures $T = 340$ K and the growth of the films was monitored by medium-energy electron-diffraction (MEED). The intensity oscillations of the specular spot for all three layers, which were recorded during the evaporation process, are shown in Fig. 2 for the $\text{Ni}_7/\text{Cu}_{4.3}/\text{Co}_2/\text{Cu}(001)$ trilayer (to indicate our trilayers we use the convention of giving the thickness in ML's for each individual layer as index). First 2 ML's of Co are deposited [Fig. 2(a)]. The two oscillations clearly show the good layer-by-layer growth. In the next step the Cu spacer of 8.2-ML thickness is evaporated [Fig. 2(b)]. The MEED intensity oscillations show a rapid decrease in amplitude, indicating a three-dimensional (3D) growth, which is well known even for the growth of Cu on Cu(001).¹⁶ In order to make the surface as flat as possible for the growth of the Ni film, the Cu spacer was annealed for 5 min up to 400 K. This treatment cannot produce intermixing because the surface energy of Cu is lower than the one of Co and therefore Cu tends to stay on the surface. The flatness of the top Cu layer is confirmed by the fact that during the deposition of the Ni film on top of the spacer layer [Fig. 2(c)] again one can see well defined oscillations up to 7 ML's. In summary, Fig. 2 shows that all layers grow layer-by-layer with well defined interfaces, where the maximum roughness is expected to be only 1 ML, as is well known from scanning tunneling microscopy images for annealed films like ours.¹⁷ Auger spectra taken after each preparation step did show no contamination, also not for the thickest spacer layer with 15 ML's of Cu. The fcc LEED patterns remained sharp in all cases.

Temperature-dependent FMR was measured *in situ* at 9 GHz with a commercial Varian spectrometer. The sample can be cooled down with liquid He and heated via a tungsten

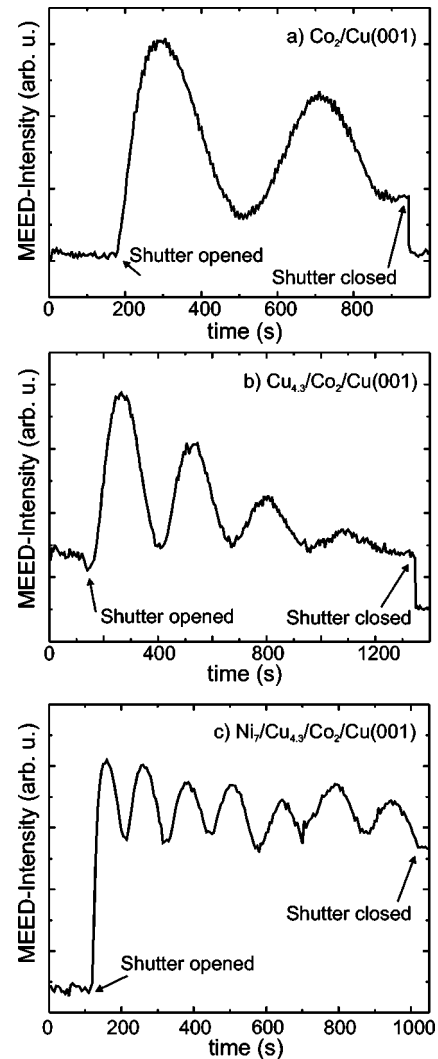


FIG. 2. Intensity of the MEED signal during the preparation of the $\text{Ni}_7/\text{Cu}_{4.3}/\text{Co}_2/\text{Cu}(001)$ trilayer.

wire. This allowed us to vary the temperature during the measurements continuously between 50 and 400 K. The UHV chamber ends up in a quartz finger into which the sample can be transferred via a manipulator. The whole quartz finger can then be inserted in a cylindrical cavity, so that all microwave components are in laboratory air.¹⁸ The cavity fits between the poles of an electromagnet which supplied the uniform dc magnetic field and is capable of generating 16 kOe. Taking the coordinate system of Fig. 1(a), the magnetic field could be rotated in the yz plane. The microwave energy produced by a klystron is coupled via wave guides into the cavity at right angles with respect to the dc magnetic field. Ideally, all the power incident upon the cavity is coupled into it and therefore none is reflected back. However, when the spin system of the sample absorbs microwave power, an FMR signal is produced which changes the impedance of the cavity thus generating a small signal component to be reflected from the cavity. With the help of a diode the variation of the reflected microwave power as a function of the magnetic field—the absorption curve—is measured. The FMR signal is amplified by weakly modulating the applied

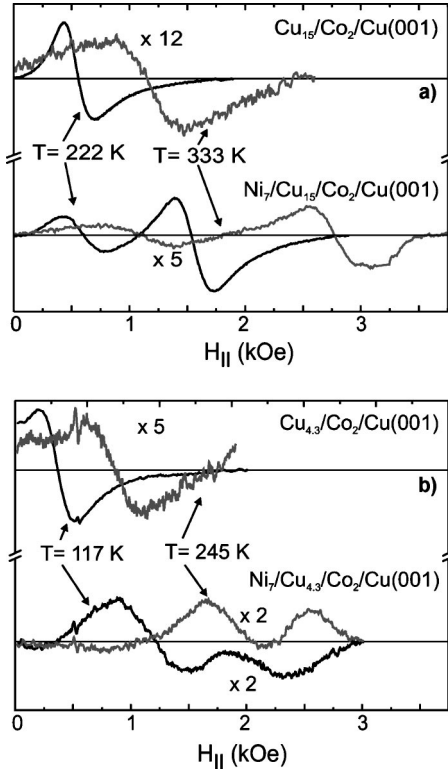


FIG. 3. The in-plane FMR signals, being the derivative of the microwave power absorption with respect to the external magnetic field, are plotted for the trilayer with the thickest $[\text{Ni}_7/\text{Cu}_{15}/\text{Co}_2/\text{Cu}(001)]$, see (a) and the thinnest $[\text{Ni}_7/\text{Cu}_{4.3}/\text{Co}_2/\text{Cu}(001)]$, see (b) Cu spacer layer. In each figure we show for two different temperatures the single (top) and coupled (bottom) FMR. The gain levels given as multiplication factors at the spectra are with respect to the signal of the uncoupled systems, i.e., with respect to the single FMR at $T=222$ K in Fig. 3(a), whereas in Fig. 3(b) all factors refer to the single FMR at $T=117$ K.

dc field at 100 kHz and detecting the 100-kHz component of the signal with a lock-in amplifier. Therefore we measure the first derivative of the absorption curve with respect to the dc magnetic field. In the ultrathin film limit, i.e., for the case that the magnetic structures are thin compared to the skin depth of the microwave, the line shape of the absorption curve is almost purely Lorentzian. This was also shown theoretically.¹⁹

The FMR measurements were performed in two steps: First the Co film capped with the Cu spacer was investigated. In the second step the Ni film was prepared and the exchange coupled trilayer system was measured and compared to the uncoupled case.

EXPERIMENTAL RESULTS AND DISCUSSION

Resonance fields

In Fig. 3 the in-plane FMR spectra measured with the FMR spectrometer described in Sec. III are shown for the thickest Cu spacer of 15 ML's [Fig. 3(a)] and the thinnest spacer of 4.3 ML's [Fig. 3(b)]. For each case the FMR for the Cu capped single Co film only (upper panel) and the

coupled Ni/Co films (lower panel) are plotted. The experimental spectra are presented for two different temperatures.

Uncoupled case: The FMR spectra for the uncoupled cases (top panels) are discussed first. As can be seen in the top panel of Fig. 3(a), the resonance field H_{res} of the single 2-ML Co film capped with 15-ML Cu moves to higher field values for the higher temperature of $T=333$ K. In addition the intensity of the signal is reduced because of the reduction in the spontaneous magnetization M . To make the peak-to-peak amplitude nearly equal to the one at 222 K, for better illustration, the signal is multiplied by a factor of 12. This explains also the higher noise level of the signal at 333 K. One should note that the FMR intensity is proportional to the spontaneous magnetization and, for a Lorentzian, is given by the product of the peak-to-peak amplitude and the linewidth squared. Since for higher temperatures the peak-to-peak amplitude decreases, whereas the linewidth increases, a reduction in the peak-to-peak amplitude by a factor of 12 does not mean that also M is reduced by that factor. The top panel of Fig. 3(b) shows that the same behavior is found also for 2 ML's of Co capped only with 4.3 ML's of Cu.

To understand the increase of H_{res} as a function of the temperature one has to note that in the paramagnetic limit, no internal fields such as anisotropy fields or demagnetizing fields are present or they are at least very small. Following Smit and Beljers,¹³ the dispersion relation is now simply given by

$$\frac{\omega}{\gamma} = H. \quad (8)$$

$\gamma = g\mu_B/\hbar$ is the gyromagnetic ratio, g is the g value, and μ_B is the Bohr magneton. Using the bulk Co value $g = 2.18$ and the microwave frequency of $\omega = 9$ GHz in the dispersion relation, one ends up with a field value of $H = 2.98$ kOe, which is the resonance field for an isotropic Co film above the Curie temperature T_C . Below T_C and for our case in which the external field is applied along the easy axis of the Co film, the internal effective field acting on the spins is equal to the sum of the external field H and the anisotropy field H_A so that both fields enter in the resonance condition (8). As a consequence for the same frequency the resonance field H_{res} has to be below the isotropic value of 2.98 kOe. Since with increasing temperature the spontaneous magnetization as well as the anisotropy fields in the film decrease, H_{res} increases towards the isotropic value.

Coupled case: Now we will turn to the coupled trilayer systems. For the coupled Ni/Co trilayer with a spacer thickness of 15 ML's [lower panel of Fig. 3(a)] two resonance modes are detected for both temperatures: For the lower temperature ($T=222$ K) one mode appears approximately at the same resonance field as the former Co resonance whereas the second mode shows up at about 1.6 kOe. For the thinner Cu spacer of 4.3 ML's [Fig. 3(b)] also two resonances are observed. This time the low field mode is shifted to higher field values compared to the single Co signal while the higher field mode is observed at about 1.9 kOe. For both

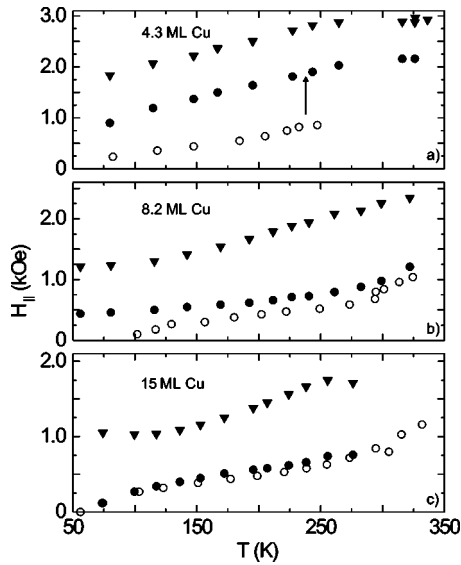


FIG. 4. The in-plane resonance fields as function of the temperature for the three different spacer thicknesses. The open circles indicate the noncoupled single layer case, the filled circles the lower field mode of the coupled case after the deposition of the Ni film. The filled triangles show the resonance position of the second mode in the trilayer. The arrow in the upper plot indicates the shift of the Co signal.

spacer thicknesses the behavior as a function of the temperature is the same as discussed for the case of the single Co film.

As discussed in Sec. II it is possible to extract the sign of the coupling from the direction of the field shift. In order to discuss this point, the shift is shown more precisely in Fig. 4, where the various resonance fields versus temperature are plotted for all three thicknesses of the Cu spacer (4.3, 8.2, 15 ML's). The open symbols correspond to the single Co film and the full symbols to the coupled Ni/Co trilayers. For the case of the 15-ML Cu spacer the shift of the resonance position is very small, while with decreasing thickness of the Cu spacer to 8.2 and 4.3 ML's the signal shifts to higher fields. For 8.2 ML's the shift is 0.18–0.35 kOe depending on the temperature, whereas for the 4.3-ML spacer it is 0.66–1.1 kOe.

According to the theory of coupled systems (Sec. II) the two signals originate from both layers. Like for coupled pendula both eigenmodes are different from the noncoupled case. As a consequence it is not possible anymore to assign the resonances to the single Co or Ni layer. For the thickest spacer, however, the coupling strength is very small,²⁰ the shift of the Co signal is small within the error bars and therefore the trilayer is nearly decoupled. In such a case it is possible to attribute the signal at lower fields to the Co layer and the one at higher fields to the Ni layer. If we now turn to the intermediate spacer thickness of 8.2 ML's, both lines shift to higher fields, indicating antiferromagnetic coupling according to the discussion in Sec. II. In a straightforward way one has to identify the lower field signal with the *acoustic mode*, the higher field signal with the *optic mode*. The same type of coupling can be seen for the thinnest spacer of

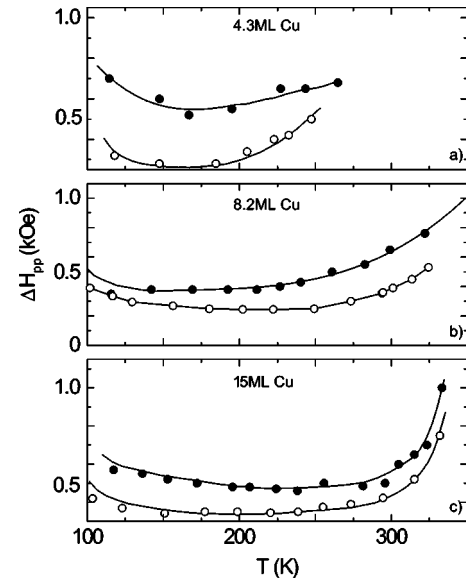


FIG. 5. The in-plane linewidths as function of the temperature for the three different spacer thicknesses. The symbols have the same meaning as in Fig. 4 and the line is a guide to the eye.

4.3 ML's. Since the shift is much stronger, the coupling strength increases. Bruno and Chappert have calculated the oscillatory behavior of the interlayer exchange coupling as function of the spacer thickness.²⁰ The calculations were also done for nonideal, i.e., rough, interfaces with 50% of the spacer being N layers thick and 25% having thicknesses of $N-1$ and $N+1$, respectively. This ± 1 ML of roughness could be reasonable for our samples (see the experimental part).¹⁷ According to Ref. 20 the antiferromagnetic maxima should be found at about 4.5, 9, and 15 ML's which is in very good agreement with our experimental findings.

Figures 3 and 4 show the capability of FMR to study the interlayer exchange coupling of our model-type Ni/Co trilayers. Moreover, the *in-situ* preparation demonstrates in a direct way the effect of interlayer exchange coupling on the magnetic properties of an individual single film (open symbols versus full symbols in Fig. 4).

Linewidth

FMR can be used to study magnetic ground-state properties of single and multilayer films. But in most investigations the linewidths of the FMR signals have almost not been discussed. In a previous publication we have shown²¹ that besides the importance of the resonance position, the width of the resonance signal can give very valuable information on the magnetic properties. Inhomogeneities in the magnetic film can add an extra inhomogeneous contribution to the linewidth. However, we will show that the main effect on the linewidth is due to the *homogeneous*, i.e., the intrinsic, contribution. Besides the usual damping mechanisms that influence the linewidth and have been discussed for single films,²¹ the coupling between the layers gives also rise to a change of the linewidths of the coupled FMR modes.²

Figure 5 shows the evolution of the linewidth as a function of the temperature for our films. The signal of the low-

field resonance in the coupled case and the Co signal for the single layer film are compared.

Uncoupled case: First the single layer case, i.e., the Co signal, is discussed in order to summarize the main mechanisms that influence the linewidth. (i) For all spacer thicknesses one observes an increase of the linewidth in the region close to the Curie temperature T_C . This behavior can be understood in terms of the intrinsic damping,²¹

$$\Delta H_{pp} = \frac{2}{\sqrt{3}} \frac{G}{\gamma^2 M} \cdot \omega. \quad (9)$$

Here G denotes the Gilbert-damping parameter, γ is the gyromagnetic ratio, and ω the microwave frequency. Since near T_C the magnetization becomes small due to fluctuations, the linewidth increases. (ii) Below T_C a shallow minimum of ΔH_{pp} is found. (iii) For even lower temperatures deep in the ferromagnetic regime the linewidth shows usually a small increase. Qualitatively, this can be understood as an inhomogeneous broadening. Since the anisotropy constants are strongly temperature dependent and increase with decreasing temperature,⁹ a variation of say 1% causes a larger inhomogeneous linewidth for lower temperatures. Since the increase at lower temperatures in our films is obviously small (Fig. 5), we have to conclude that the inhomogeneous contribution to the linewidth is small in our case.

Coupled case: In the coupled cases for 15- and 8.2 ML spacer thickness the behavior as a function of the temperature is similar compared to the single layer films, but the linewidth nearly doubles after the coupling is introduced. In a simple picture this can be understood in the following way: Both ferromagnetic layers have different damping parameters for the general situation of the asymmetric trilayer. In the uncoupled case the larger the intrinsic damping, the larger will be the linewidth. If these layers become coupled, the magnetization of the layer with larger damping will relax slower during resonance, because it can transfer energy to the other layer, which has a smaller damping parameter. For stronger coupling this transfer of energy is more effective and therefore the increase of the linewidth will be larger. As a consequence the line that was broader in the uncoupled case becomes smaller. This argument consequently predicts that the line which was smaller before the coupling is intro-

duced becomes broader in the coupled system. This scenario is supported by calculations of the FMR linewidths in coupled trilayers.² In our trilayers the Co signal has, in the uncoupled case, the smaller Gilbert damping parameter and by introducing the coupling this resonance becomes the acoustic mode. Since the linewidth of the acoustic mode broadens in comparison to the Co signal in the single layer film, our results verify the predictions made by theory² in a direct way, because the broadening could be monitored directly. In addition, we indeed find that for thinner spacers, i.e., stronger coupling, the increase of the linewidth is larger. Another interpretation of the increase could be an inhomogeneous broadening due to a lateral distribution of the film thickness, which would lead to a variation of the coupling strength J_{AB} across the film plane. However, for the uncoupled films we have found that the inhomogeneous contribution to the overall linewidth is small. This and the systematic increase of the linewidth makes the interpretation assuming an inhomogeneous broadening *only* very unlikely. Therefore, in agreement with the theory,² we attribute the main effect to an intrinsic broadening due to coupling.

CONCLUSION

Via FMR we have studied the magnetic properties of ultrathin fcc Ni/Cu/Co trilayer structures grown on Cu(001) between 40 and 400 K. For the first time the measurements could be done *in-situ*. Therefore it was possible to compare the coupled trilayer with the uncoupled Cu capped Co system. Consistent with theory we have observed two FMR signals, corresponding to the optic and acoustic mode. Due to coupling a shift of the resonance field compared to the capped Co film was found which becomes larger for smaller spacer thicknesses, i.e., for stronger coupling. In addition we have measured an increase of the linewidth of the Co signal after introducing the coupling, which shows that not only the static but also the dynamical properties of the magnetization, i.e., the intrinsic damping mechanisms, are influenced when one couples two ferromagnetic elements with different damping parameters.

ACKNOWLEDGMENT

This work was supported by the DFG, Sfb 290.

*Corresponding author.

[†]Present address: Institut für Halbleiterphysik und Optik, Technische Universität Braunschweig, Mendelssohnstr. 3, D-38106 Braunschweig, Germany.

¹J. J. Krebs, P. Lubitz, A. Chaiken, and G. A. Prinz, Phys. Rev. Lett. **63**, 1645 (1989).

²A. Layadi and J. O. Artman, J. Magn. Magn. Mater. **92**, 143 (1990).

³B. Heinrich, J. F. Cochran, M. Kowalewski, J. Kirschner, Z. Celinski, A. S. Arrot, and K. Myrtle, Phys. Rev. B **44**, 9348 (1991).

⁴P. E. Wigen and Z. Zhang, Braz. J. Phys. **22**, 267 (1992).

⁵Z. Zhang, L. Zhou, P. E. Wigen, and K. Ounadjela, Phys. Rev. B **50**, 6094 (1994).

⁶Y. Roussigné, F. Ganot, C. Dugautier, P. Moch, and D. Renard,

Phys. Rev. B **52**, 350 (1995).

⁷A. Azevedo, C. Chesman, S. M. Rezende, F. M. de Aguiar, X. Bian, and S. S. P. Parkin, Phys. Rev. Lett. **76**, 4837 (1996).

⁸S. M. Rezende, C. Chesman, M. A. Lucena, A. Azevedo, and S. S. P. Parkin, J. Appl. Phys. **84**, 958 (1998).

⁹M. Farle, Rep. Prog. Phys. **61**, 755 (1998).

¹⁰J. J. de Vries, A. A. P. Schudelaro, R. Jungblut, P. J. H. Bloemen, A. Reinders, J. Kohlhepp, R. Coehoorn, and W. J. M. de Jonge, Phys. Rev. Lett. **75**, 4306 (1995).

¹¹H. P. Oepen, M. Benning, H. Ibach, C. M. Schneider, and J. Kirschner, J. Magn. Magn. Mater. **86**, L137 (1990).

¹²B. Schulz and K. Baberschke, Phys. Rev. B **50**, 13 467 (1994).

¹³J. Smit and H. G. Beljers, Philips Res. Rep. **10**, 113 (1955).

¹⁴B. Heinrich and J. A. C. Bland, *Ultrathin Magnetic Structures II*

- (Springer-Verlag, Berlin, 1994).
- ¹⁵M. Ritter, M. Stindtman, M. Farle, and K. Baberschke, *Surf. Sci.* **348**, 243 (1996).
- ¹⁶J.-K. Zou and J. F. Wendelken, *Phys. Rev. Lett.* **78**, 2791 (1997).
- ¹⁷J. Shen, M.-T. Lin, J. Giergiel, C. Schmidthals, M. Zharnikov, C. M. Schneider, and J. Kirschner, *J. Magn. Magn. Mater.* **156**, 104 (1996).
- ¹⁸M. Farle, M. Zomack, and K. Baberschke, *Surf. Sci.* **160**, 205 (1985).
- ¹⁹Z. Celinski, K. B. Urquhart, and B. Heinrich, *J. Magn. Magn. Mater.* **166**, 6 (1997).
- ²⁰P. Bruno and C. Chappert, *Phys. Rev. Lett.* **67**, 1602 (1991).
- ²¹W. Platow, A. N. Anisimov, G. L. Dunifer, M. Farle, and K. Baberschke, *Phys. Rev. B* **58**, 5611 (1998).